



Joint PP-PS model building for complex geology – an example from Offshore Mexico

John Mathewson and Miguel Acosta Perez, WesternGeco; Edgar Serrano Casillas, Silvino Dominguez Garcia, and Jorge Diaz de Leon Chagolla, PEMEX*

Summary

PS converted-wave seismic data is beneficial in many situations, such as those where images are distorted by the presence of shallow gas, or to improve estimation of density and shear impedance in seismic inversion. However, processing both PP and PS data naturally requires more effort than processing of PP data alone, and for this reason much PS data remains unprocessed. Efficient workflows for processing of PS seismic data are required to minimize the extra time required for PS processing.

Model building for depth imaging of PS data is more complicated than for PP data because both compressional and shear velocities are required, and both data types must be input. However, these extra requirements are not only a complication, but also provide an opportunity to build better models that satisfy all input data in a joint PP-PS tomography.

In this case study, we describe the application of PP-PS model building and depth imaging to an ocean-bottom cable seismic survey in the southern Gulf of Mexico. The area is characterized by complex structure combined with large velocity contrasts, both of which are problematic for PS model building. We applied a state-of-the-art workflow incorporating joint PP-PS tomography that maximized use of well data and required very little interpretation effort. High-quality PP and PS results were produced in a reasonable timeframe.

Introduction

The southern Gulf of Mexico has been a source of significant quantities of petroleum for many years. Huge reserves remain, but production rates in older fields have decreased over time. Efforts are being made to extend the life of these fields, and improved seismic data is an important part of these efforts. Recently an ocean-bottom cable (OBC) survey was acquired using high-density orthogonal acquisition, with high fold and long-offset coverage over 360° of azimuth. Seismic data from the new OBC survey are greatly superior to data from previous surveys in the area in terms of bandwidth, signal-to-noise ratio, and full-offset/azimuth illumination.

The main objective of this survey was to produce better PP seismic volumes that will reduce structural uncertainty, suitable for fracture characterization and analysis of seismic attributes. However, horizontal components were recorded during acquisition and these were also processed to produce PS converted-wave images. Reasons for processing the PS data include improved imaging in areas affected by shallow gas as well as potential benefits for reservoir characterization, geomechanics and rock physics.

Velocity model building was carried out using an advanced workflow featuring multiple iterations of joint PP-PS common image point (CIP) tomography with floating event constraints performing simultaneous updates of V_p , V_s and anisotropic parameters (Mathewson et al., 2013). The workflow incorporated extensive use at

every stage of the large amount of high-quality well data available in the project area, minimal interpretation requirements for model building, and use of surface-wave inversion to define shallow shear-wave velocity.

Initial model for PP-PS depth imaging

Model building for imaging of PS seismic data is complicated by the requirement for both P-velocity and S-velocity, and by the greater sensitivity of PS imaging to errors in anisotropic parameters. In our case, we were fortunate to have a high-quality tilted transversely isotropic (TTI) model produced during an earlier phase of the project using iterations of PP CIP tomography (Woodward et al., 2008) with well constraints. V_p , anisotropic parameters and TTI dip and azimuth were all extracted from this model to form the initial model for PS depth imaging.

Creation of the initial S-velocity model was greatly aided by the availability of many wells with dipole sonic logs sampling the entire Tertiary section as well as Mesozoic carbonates and Jurassic layers. A crossplot of V_p and V_s from dipole sonic data was used to derive a V_p/V_s relationship, which was then used to calculate V_s from the initial V_p model.

Determination of shear velocities using reflections in the very shallow section is problematic given the sparse shallow illumination of orthogonal OBC acquisition and the lack of shallow well data. Surface-wave inversion (Boiero et al., 2013) was performed to resolve V_s variations just below the water bottom. Figure 1 shows depth-migrated sections produced with and without velocities from surface-wave inversion. A false shallow structure is apparent in the image on the left, which is totally removed by V_s updates based on surface-wave inversion.

Figure 2 shows a depth-migrated PS section with color overlay of the initial V_s model. The image is of very good quality given that this is the initial model. Large velocity contrasts and complicated structure are clearly seen.

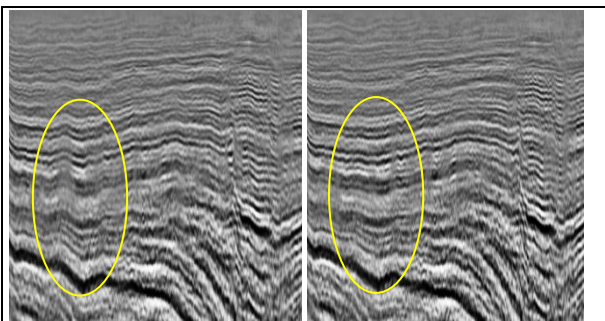


Figure 1: Depth-migrated sections without (left) and with (right) shallow shear velocity from surface wave inversion.

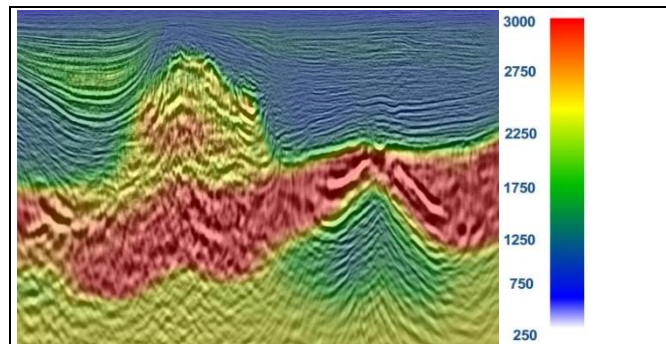


Figure 2: Initial PS depth-migrated section with V_s model overlaid.

Modeling carbonate velocities

Velocities of the Mesozoic carbonates are significantly higher than the Tertiary section, and some modeling was required to include the large velocity contrasts in the model. Image-guided interpolation (Hale, 2010) is an efficient way to interpolate sparse input data using structural input from an image. VSP and sonic log data for over 100 wells were interpolated using this method to produce a detailed P-velocity model below the top of the high-velocity carbonate layer. Following this interpolation, the shear velocity model was recalculated below the top carbonate, using the V_p/V_s ratio derived from well logs applied to the updated

compressional velocity. Artificial wells were inserted in some locations where no well information was available, as well as to guide interpolation in a couple of particularly complex areas.

Figure 3 shows the image and model before and after carbonate velocity modeling with image-guided interpolation of the well velocity data. After the update, we see increased velocity in the allochthonous carbonates with velocity inversion below. The velocity changes have improved continuity and we also have a more reasonable structure of deeper events for both PP and PS images.

Joint PP-PS tomography

Joint PP-PS tomography (Mathewson et al., 2013) is a robust algorithm in which residual moveout picks for PP and PS depth gathers are combined with floating event constraints in ray-trace CIP tomography. It is capable of solving simultaneously for V_p , V_s , and anisotropic parameters δ and ϵ (Thomsen, 1986). It provides better estimates of anellipticity than either PP data alone or separate PP and PS updates, as well as a more accurate V_p/V_s ratio for an improved PP-PS match. It should be noted that updating of δ requires well depth constraints.

A key part of the joint tomography is the inclusion of the relative shift between PP and PS depth images. These images should tie each other, although the tie may not be obvious. For example, PP and PS reflectivity can be very different and there may be a difference in phase between images. To understand the PP-PS tie, we produced synthetic seismograms from dipole sonic log data calibrated with checkshot information.

Analysis of the PP and PS synthetics led us to conclude that the images should tie with opposite polarity. In Figure 4 are displays of the PP and PS synthetic ties at one of the wells. The most obvious feature is the high-velocity zone in the center of the displayed interval. For PP data this produces a positive reflection coefficient at the top and negative at the bottom, while PS has a negative reflection at the top and positive at the bottom.

We applied a preconditioning flow consisting of high-cut filtering of PP and PS depth images and polarity reversal of the PS data. Dynamic warping was then applied (Hale, 2013) to automatically determine the spatially varying displacement between PP and PS depth volumes for input to joint tomography. In general, PP and PS depths matched closely but in some places there were vertical shifts up to 400m. Dynamic warping is particularly resistant to cycle-skipping and was able to successfully resolve the largest shifts.

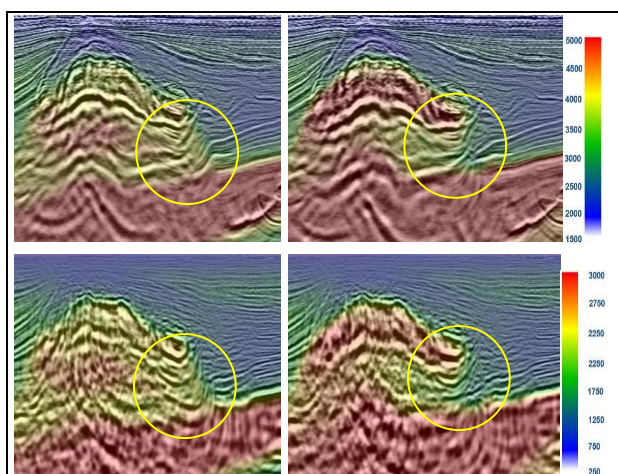


Figure 3: PP (top) and PS (bottom) images with model overlay before (left) and after (right) modeling of carbonate velocities.

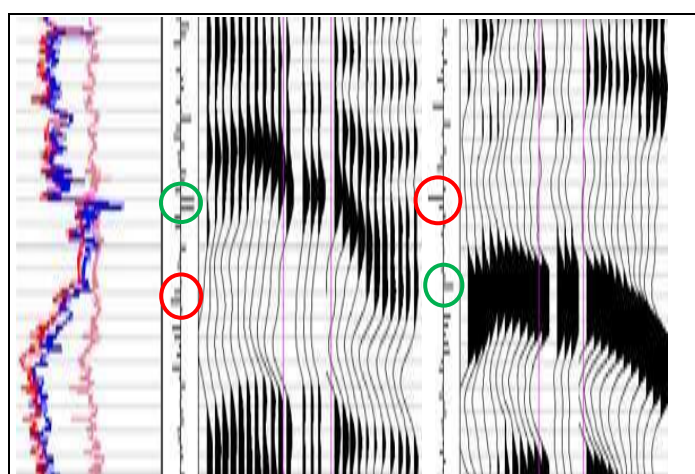


Figure 4: V_p , density and acoustic impedance (left), PP (middle) and PS (right) reflectivity and synthetic tie.

Iterations of Joint PP-PS tomography were performed to simultaneously update V_p , V_s , δ , and ϵ . A combination of vertical seismic profile (VSP) travel-times, sonic logs, and well marker/horizon misties was used to constrain the solutions. For each iteration of tomography, floating-event constraints relating depths in PP and PS images were included, and these came from a PP-PS displacement field derived using dynamic warping with no interpretation input. Model updates for each iteration of joint PP-PS tomography produced flatter events, better PP-PS match, improved well misties and better agreement with sonic logs and checkshots, compared with the input model.

Results

After completion of the Joint PP-PS model building workflow, depth imaging was performed. Figure 5 shows PP and PS depth images for an inline migrated using the final model. The two images look very similar, as they should. They show the same geology. The PS image is very interpretable, even in structurally complex areas below the carbonate, although it has a somewhat higher noise level and lacks higher frequencies that are present in the PP image. Depth gathers from the right side of the same inline are displayed as butterfly gathers in Figure 6. Traces on the left side of each gather are PS data while the right side is PP. There is a nearly perfect match between the PP and PS data to the base of the high-velocity carbonate, although the PS data is inferior in the deeper section. Residual moveout on events down to the base carbonate is minimal for both PP and PS data, even at far offsets.

Figure 7 shows V_p and V_s functions calculated from dipole sonic logs at two well locations, along with the V_p/V_s ratio calculated by dividing the two functions. In the well on the left, dipole sonic data were only acquired in the Tertiary section, whereas for the well on the right they were only acquired in the carbonate section. VSP interval velocity is also displayed for both wells. V_p , V_s , and V_p/V_s ratio from the final model are also displayed and match very closely with the dipole sonic information as well as the VSP data.

Conclusions

We applied PP-PS model building and depth imaging on a recently acquired full-azimuth OBC data set from offshore Mexico. We employed an innovative model building workflow, using the latest technologies to extract maximum information from both PP and PS seismic data and the large amount of well data in the area. The resulting model matches closely with well data and produces excellent PP and PS depth images that tie. Model building turnaround was very reasonable considering the complex geology and large spatial velocity variations.

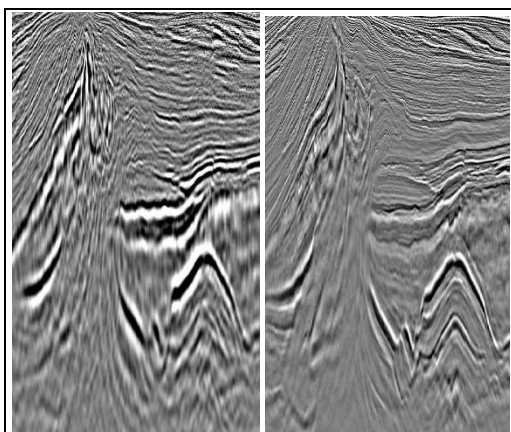


Figure 5: Example of final PS (left) and PP (right) depth images.

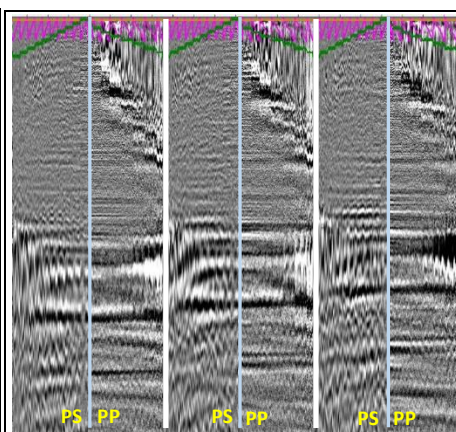


Figure 6: Example of final butterfly depth gathers, PS on the left of each gather and PP on the right. Azimuth (magenta) and offset (green) are graphed at the top of the display.

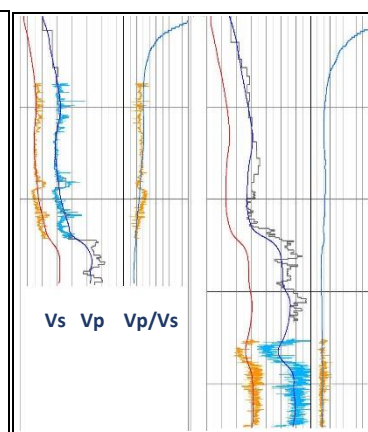


Figure 7: Comparison display at two wells of V_s (orange), V_p (blue), and V_p/V_s ratio from the final velocity model with dipole sonic log data.

References

Boiero, D., Wiarda, E., and Vermeer, P. [2013] Surface- and guided-wave inversion for near-surface modeling in land and shallow marine seismic data. *The Leading Edge*, 32(6), 638-646.

Hale, D. [2013] Dynamic warping of seismic images. *Geophysics*, 78(2), S105-S115.

Hale, D. [2010] Image-guided 3D interpolation of borehole data. 70th Annual International Meeting, SEG Expanded Abstracts, 1266-1270.

Mathewson, J., Woodward, M., Nichols D., Xu, C., and Leone, C. [2013] Joint PP/PS tomography with floating event constraints. 83rd Annual International Meeting, SEG Expanded Abstracts, 1649-1653.

Thomsen, L. [1986] Weak elastic anisotropy. *Geophysics*, 51(10), 1954–1966.

Woodward, M., Nichols, D., Zdraveva, O., Whitfield, P., and Johns, T. [2008] A decade of tomography. *Geophysics*, 73(5), VE5–VE11.